

Molecular Gas in the Perseus Cooling Flow Galaxy, NGC 1275

Terry J. Bridges^{1,2,4} and Judith A. Irwin^{3,5}

¹*Royal Greenwich Observatory, Madingley Road, Cambridge, England, CB3 0EZ*

²*Institute of Astronomy, Madingley Road, Cambridge, England, CB3 0HA*

³*Department of Physics, Queen's University, Kingston, Ontario, Canada, K7L 3N6*

⁴*E-mail: tjb@ast.cam.ac.uk*

⁵*E-mail: irwin@astro.queensu.ca*

Accepted . . . Received

ABSTRACT

The central arcminute of the Perseus cooling flow galaxy, NGC 1275, has been mapped with the JCMT in $^{12}\text{CO}(2-1)$ at $21''$ resolution, with detections out to at least $36''$ (12 kpc). Within the limits of the resolution and coverage, the distribution of gas appears to be roughly E-W, consistent with previous observations of CO, X-ray, $\text{H}\alpha$, and dust emission. The total detected molecular hydrogen mass is $\sim 1.6 \times 10^{10} M_{\odot}$, using a Galactic conversion factor. The inner central rotating disk is apparent in the data, but the overall distribution is not one of rotation. Rather, the line profiles are bluewards asymmetric, consistent with previous observations in HI and [OIII]. We suggest that the blueshift may be due to an acquired mean velocity of $\sim 150 \text{ km s}^{-1}$ imparted by the radio jet in the advancing direction. Within the uncertainties of the analysis, the available radio energy appears to be sufficient, and the interpretation is consistent with that of Bohringer et al. (1993) for displaced X-ray emission.

We have also made the first observations of $^{13}\text{CO}(2-1)$ and $^{12}\text{CO}(3-2)$ emission from the central $21''$ region of NGC 1275 and combined these data with IRAM data supplied by Reuter et al. (1993) to form line ratios over equivalent, well-sampled regions. An LVG radiative transfer analysis indicates that the line ratios are not well reproduced by a single value of kinetic temperature, molecular hydrogen density, and abundance per unit velocity gradient. At least two temperatures are suggested by a simple two-component LVG model, possibly reflecting a temperature gradient in this region.

Key words: galaxies: individual:NGC 1275- galaxies: clusters: individual: Perseus-cooling flows-galaxies:ISM-CO:galaxies- radiative transfer

1 INTRODUCTION

Cluster cooling flows present a most intriguing conspiracy. X-ray observations have revealed large quantities of hot, diffuse gas in most if not all clusters (e.g. Fabian 1994). In many clusters (70–90%) the central gas densities are high enough that the radiative cooling time becomes shorter than the Hubble time (e.g. Edge, Stewart, & Fabian 1992; Fabian 1994). Thus pressure-driven cooling flows are inferred. In several clusters, soft X-ray emission has also revealed the presence of gas at intermediate temperatures of 10^5 – 10^7 K, as would be expected for gas condensing out of a cooling flow (e.g. Johnstone et al. 1992). If the inferred mass deposition rates of between 10–1000 M_{\odot} are maintained over a

Hubble time, then $\sim 10^{12} - 10^{13} M_{\odot}$ of material should be deposited in the cores of clusters.

However, there is little evidence for all of this supposed infalling material at other wavelengths. Optical data apparently rule out star formation with a ‘normal’ (ie. Galactic) mass function (e.g. McNamara & O’Connell 1992). Some fraction of the cooling material should exist in cool atomic and/or molecular clouds. However, HI emission has not been detected in any cooling flow cluster, with upper limits of 10^9 – $10^{10} M_{\odot}$, while HI has been detected in absorption in only four clusters (e.g. Jaffe 1992). As well, Annis & Jewitt (1993) carried out an unsuccessful search for thermal emission from cold dust in 11 clusters, placing upper limits of $\sim 10^{10} M_{\odot}$ on the mass of cold gas in these clusters, assuming a Galactic gas/dust ratio. Searches for molecular gas (ie.

CO) have also been unfruitful, with one exception (see below) in over a dozen clusters (e.g. Grabelski & Ulmer 1990; McNamara & Jaffe 1994); again typical upper limits to the H_2 mass are $\sim 10^{10} M_\odot$.

The only cooling flow galaxy in which CO has yet been detected is the one in the Perseus Cluster (Abell 426) for which infall rates of $\sim 300\text{--}500 M_\odot$ per year centered on the giant cD galaxy, NGC 1275, have been inferred (Gorenstein et al. 1978; Fabian et al. 1981; Mushotzky et al. 1981; Allen et al. 1992; Allen & Fabian 1997). Allen & Fabian (1997) find excess X-ray absorption from ROSAT data in the central $30''$ of the cluster implying a total mass of $\sim 4 \times 10^8 M_\odot$. A system of $H\alpha$ filaments extending to $\approx 2' = 40$ kpc from the core of NGC 1275 has been linked to the cooling gas (Lynds 1970; Cowie, Fabian, & Nulsen 1980; Heckman et al. 1989). NGC 1275 is also home to the highly variable radio source 3C84 (e.g. Pedlar et al. 1990). HI, in quantities of $\sim 10^{10} M_\odot$, has been detected in absorption against this source (Jaffe 1990) and the relativistic outflow appears to be displacing X-ray emitting gas on arcminute scales (Bohringer et al. 1993). A foreground infalling ($\Delta V \approx 3000 \text{ km s}^{-1}$) system is also known to exist (Minkowski 1957; Lynds 1970; Hu et al. 1983; Caulet et al. 1992) and there is some evidence that NGC 1275 has experienced a previous merger (e.g. Holtzman et al. 1992). Braine et al. (1995) attribute the origin of the molecular gas in NGC 1275 to a previous merger as do Lester et al. (1995) for the origin of the $100 \mu\text{m}$ emitting dust.

Previous CO observations of NGC 1275 include single-dish detections by Lazareff et al. (1989), and Mirabel, Sanders, & Kazes (1989), as well as a partial mapping by Reuter et al. (1993) to $\sim 20''$ radius in $^{12}\text{CO}(1-0)$ and $^{12}\text{CO}(2-1)$ with the Institut de Radioastronomie Millimétrique (IRAM) telescope. Estimated H_2 masses are of order $M_{H_2} \sim 10^{10} M_\odot$ using Galactic CO to H_2 conversion factors. High resolution $^{12}\text{CO}(1-0)$ interferometry has now also been carried out by Braine et al. (1995) and Inoue et al. (1996). The latter authors find a rotating ring-like CO structure with a ring radius of $3.5''$. A hot ($T = 1700 \text{ K}$) component of molecular hydrogen has also been directly detected through $2 \mu\text{m}$ emission within the central few arcseconds (Fischer et al. 1987; Kawara & Taniguchi 1993; Inoue et al. 1996). No attempt has yet been made to determine the physical properties of the molecular gas in this most unusual system.

In this paper, we present $^{12}\text{CO}(2-1)$, $^{13}\text{CO}(2-1)$, and $^{12}\text{CO}(3-2)$ observations of NGC 1275 using the 15 m James Clerk Maxwell Telescope (JCMT). We have mapped the galaxy in the $^{12}\text{CO}(2-1)$ line out to ~ 1 arcmin and in the $^{12}\text{CO}(3-2)$ line out to ~ 14 arcsec. In addition, we have obtained IRAM $^{12}\text{CO}(2-1)$ and $^{12}\text{CO}(1-0)$ data, kindly supplied by Reuter et al. (1993). Together with the JCMT data, we perform a line ratio analysis for the central position in order to constrain the physical conditions in the molecular gas and see whether these are consistent with a cooling flow origin. The observations are described in Section 2, the results are presented in Section 3, the line ratio analysis is discussed in Section 4, some physical quantities are derived in Section 5, there is a Discussion in Section 6, and our main conclusions are summarized in Section 7. For NGC 1275, we take $D = 70 \text{ Mpc}$, ($cz = 5250 \text{ km s}^{-1}$; $H_0 = 75 \text{ km s}^{-1} \text{ Mpc}^{-1}$) in which case $1'' = 340 \text{ pc}$.

2 OBSERVATIONS AND DATA REDUCTION

$^{12}\text{CO}(2-1)$ and $^{13}\text{CO}(2-1)$ data were obtained during 3 shifts at the JCMT* on Mauna Kea during 23–25 November 1994. The beam-size at 230 GHz ($^{12}\text{CO}(2-1)$) is $21''$ and is $22''$ at 220 GHz ($^{13}\text{CO}(2-1)$), which corresponds to ~ 7 kpc for $H_0 = 75 \text{ km s}^{-1} \text{ Mpc}^{-1}$. From scans of Saturn, the main-beam efficiency, η_{mb} , for $^{12}\text{CO}(2-1)$ and $^{13}\text{CO}(2-1)$ were determined to be 0.69 ± 0.05 and 0.66 ± 0.05 respectively; these values agree well with that determined by JCMT staff between 1 Nov 1994 to Jan 30 1995 (0.69 ± 0.01 ; see JCMT WWW page). Unless otherwise indicated, all temperatures quoted below are on the main-beam brightness temperature scale T_{mb} . The system temperature T_{sys} (in T_a^* units) ranged between 500–600K for $^{12}\text{CO}(2-1)$ and 600–700K for $^{13}\text{CO}(2-1)$. Pointing was done on the central radio source 3C84, CRL2688 and Saturn several times per night. During an 8 hour run, we found rms drifts in pointing of 3–4 arcsec on average. We chose our (0,0) position to be the same as that of Reuter et al. (1993), i.e. $\alpha = 03 \text{ h } 16 \text{ m } 29.29$, $\delta = +41 \text{ } 19 \text{ } 51.9$ (1950), in order to facilitate the line ratio analysis. This position is $3.5''$ west of the galaxy center which is at the 3C84 radio core, i.e. $\text{RA}(1950) = 3^{\text{h}} 16^{\text{m}} 29.86$, $\text{DEC}(1950) = 41^\circ 19' 52''$ (Pedlar et al. 1990). The displacement is \ll the beam size.

Integrations were carried out using receiver RxA2 with the DAS in its 760 Mhz configuration ($\sim 1000 \text{ km s}^{-1}$, 0.8 km s^{-1} per channel). We beam-switched with a 1 hz chopping frequency and a $150''$ throw. CRL 2688 scans were used to check the calibration for $^{12}\text{CO}(2-1)$ and $^{13}\text{CO}(2-1)$. Two $^{12}\text{CO}(2-1)$ scans of CRL 2688 yield integrated intensities of 232 K km s^{-1} (Nov 23, T_a^* units) and 202 K km s^{-1} (Nov 25), as compared to the published value of 168 K km s^{-1} on October 20, 1994. For $^{13}\text{CO}(2-1)$ the measured and published line strengths are 42 and 46 K km s^{-1} respectively, in excellent agreement. Throughout later observing runs, we also continued to check that the (0,0) spectrum gave consistent results. We integrated for 5040 sec at the galaxy center in $^{12}\text{CO}(2-1)$ (Fig. 1), and 5520 sec in $^{13}\text{CO}(2-1)$ (Fig. 3).

Subsequent data reduction was done using the UNIX SPECX package developed by Rachael Padman. The spectra were averaged (weighted inversely by T_{sys}), 20-channel binned (giving a final velocity resolution of 16.25 km s^{-1}), and baseline subtracted (linear baselines were mostly used); for $^{12}\text{CO}(2-1)$ only 3720 sec of data were usable. We also carried out a partial mapping in $^{12}\text{CO}(2-1)$, with integrations ranging between 1800–3600 sec for 8 points out to 1 arcmin from the galaxy center (see below and Section 3.3 for more details). The sampling was $20''$ in RA and $15''$ in DEC with beam centers in each row displaced by $10''$ so that full coverage was obtained with the $21''$ beam, though not at the Nyquist rate.

$^{12}\text{CO}(3-2)$ observations of a 5-point (0,0; $-7,+7$; $+7,-7$; $+7,+7$; $-7,-7$) map at the center of NGC 1275 were obtained during service time on July 31 1995. The beamsize is $14''$ at 345 GHz, and $\eta_{mb} = 0.525 \pm 0.033$, as measured

* The James Clerk Maxwell Telescope is operated by the Royal Observatory, Edinburgh on behalf of the Science and Engineering Research Council of the United Kingdom, the Netherlands Organization for Scientific Research, and the National Research Council of Canada.

Table 1. Telescope Parameters

Spectral Line	Telescope	Beam FWHM	η_{mb}
$^{12}\text{CO}(1-0)$	IRAM	21''	0.67
$^{12}\text{CO}(2-1)$	IRAM	12''	0.5
$^{12}\text{CO}(2-1)$	JCMT	21''	0.69/0.61 ¹
$^{13}\text{CO}(2-1)$	JCMT	22''	0.66
$^{12}\text{CO}(3-2)$	JCMT	14''	0.53

¹ For December 1994 and December 1995 respectively

from Saturn scans. Receiver RxB3i was used with the DAS in its 760 Mhz configuration ($\sim 600 \text{ km s}^{-1}$, 0.54 km s^{-1} per channel). A total of 3000 sec at 0,0 and 2400 sec at each of the other four points was obtained. Pointing done on W3, G34.3, CRL618, and Saturn shows $\sim 3''$ drifts over the 8 hour shift. Again we have averaged, binned by 20 channels (giving a velocity resolution of 11 km s^{-1}), and baseline-subtracted.

Finally, during 7 shifts in December 1995, we extended our $^{12}\text{CO}(2-1)$ mapping by obtaining 12 further points extending out to ~ 1 arcmin from the galaxy center; integrations were typically 5400 sec (see Section 3.3). Receiver A2 was used in 750 Mhz configuration (0.8 km s^{-1} per channel), with 1 hz beamswitching and a $150''$ throw. Spectra were averaged and 20-channel binned for a final velocity resolution of 16.25 km s^{-1} . Saturn scans were again used to determine a η_{mb} value of 0.61 ± 0.05 for $^{12}\text{CO}(2-1)$ on Dec 4/5, where the uncertainty includes known random errors. The JCMT value is given as 0.69 ± 0.01 (Jan 25/96), but the uncertainty in a single measurement is closer to ± 0.07 (Per Friberg, private comm.) where changes could be due to a variety of sources, including sky variations, standing waves, uncertainties in beamsize, and errors in pointing and focussing (Henry Matthews, private comm.). Thus it is important to measure η_{mb} during each observing session, as we have done. We found the same value of η_{mb} for each of three Saturn scans over Dec 4/5. T_{sys} for $^{12}\text{CO}(2-1)$ ranged between 300–400 K (Dec 3) to 500–600 K (Dec 4/5). Pointing done on W3, 3C84 and Saturn show $\sim 3''$ rms drifts over an 8-hour shift. $^{12}\text{CO}(2-1)$ calibration was checked using scans of NGC 1275, which also allowed us to check consistency with our previous data taken in Dec 1994. Five 600 sec scans taken at 0,0 yield integrated line strengths agreeing with each other to within 25%, and also with our December 1994 data (e.g. Figure 1) to within 25%.

The IRAM data were supplied by H.-P. Reuter (private communication) and full details can be found in Reuter et al. (1993).

A summary of the spectral lines and telescope parameters is listed in Table 1.

3 RESULTS

3.1 Spectra

The $^{12}\text{CO}(2-1)$ and $^{12}\text{CO}(3-2)$ spectra are shown in Fig. 1 and 2, respectively. For point (+20,0) of Fig. 1, note that the low velocity end of the baseline has been truncated. This is because several of the individual scans at this position were centered at an offset velocity, necessitating a shift in the velocity coordinate before averaging. The non-overlapping baseline regions were then truncated, but the integrity of

the spectral line itself (based on inspection of all individual scans with full baselines) has been retained. The $^{13}\text{CO}(2-1)$ spectrum for the center position is shown in Fig. 3 with the central $^{12}\text{CO}(2-1)$ spectrum superimposed. We consider the isotopic line to be a marginal detection (cf. the similarly placed peaks and troughs in comparison to $^{12}\text{CO}(2-1)$), but given the low S/N, we place little weight upon this particular spectrum in subsequent analysis.

The strong radio source, 3C84, occurs at the (0,0) position (Pedlar et al. 1990) which has a core strength in the range 2 - 6 Jy (Braine et al. 1995; private communication to Lester 1995; Inoue et al. 1996) at 115 GHz and a total size less than 10 mas (Readhead et al. 1983), or area filling factor $< 2 \times 10^{-7}$ in our $21''$ $^{12}\text{CO}(2-1)$ beam. An inspection of the original spectra before and after binning/average shows no compelling evidence for absorption features above the noise level. This is confirmed by Braine et al. (1995) and Inoue et al. (1996), neither of whom detect any $^{12}\text{CO}(1-0)$ absorption in much smaller interferometric beams of $2''$ and $4''$, respectively.

The integrated line intensities at the measured positions, $\int T_{mb} dV$, are given in Table 2, along with the peak T_{mb} and FWHM. The quoted uncertainties take into account the noise in the spectrum and, where possible, uncertainties in baseline subtraction (note that for most spectra, both authors independently computed these values). Calibration error is not included, since it is less than these other uncertainties. The peak T_{mb} and FWHM were determined by fitting Gaussians to the line profiles. For those positions where no line was detected, 3σ upper limits are given for the peak T_{mb} and $\int T_{mb} dV$, based on the observed scatter in the spectra.

3.2 The $^{12}\text{CO}(2-1)$ Map and Velocity Field

Our most extensive observations were obtained in the $^{12}\text{CO}(2-1)$ line and a map of integrated intensities is shown in Fig. 4a. The map was made by integrating each spectrum over velocity to create a grid of $\int T_{mb} dV$ and then interpolating onto a finer grid using Langrange polynomials using the Grenoble Image and Line Data Analysis System (GILDAS) software package. Real detections are observed out to 36 arcsec (= 12 kpc) from center.

The main features in Figure 4a are an east-west elongation, a peak ~ 15 arcsec east of the galaxy center, and a smaller peak near the center itself. The east-west elongation has been observed in previous maps, i.e. the single-dish data of Reuter et al. (1993) and the interferometer data of Inoue et al. (1996). The appropriate comparison of our results is with previous single-dish $^{12}\text{CO}(2-1)$ data, i.e. that obtained by Reuter et al. at a resolution of $12''$ (their Fig. 4). They find three peaks, one at (0,0), one roughly coinciding with our strongest peak to the east, and another $\sim 13''$ to the North-West. After smoothing their data to match our $21''$ beam, the IRAM data shows a peak about $5''$ to the west of centre. Thus, there is some discrepancy between data sets in the sense that the JCMT data show a stronger peak to the east of center whereas the IRAM data show a stronger peak to the west of centre. We cannot reconcile the data sets using different baseline subtractions. Possible reasons for the discrepancy could include the different beam-size, coverage, and sampling between the two data sets. Thus the general

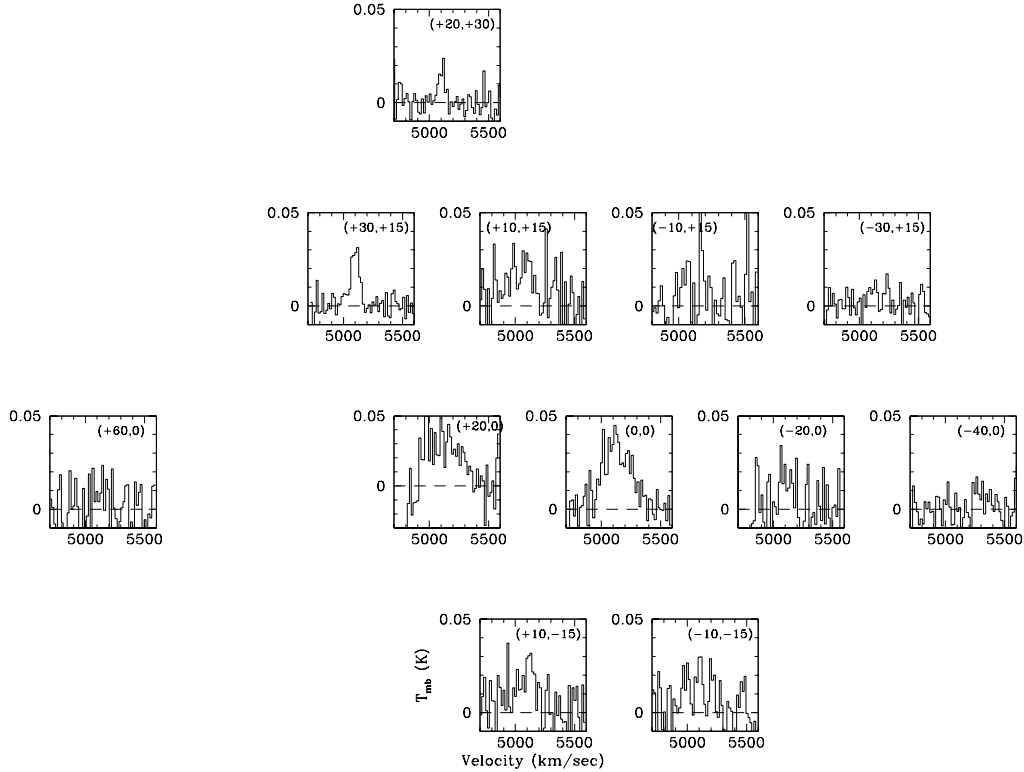


Figure 1. $^{12}\text{CO}(2-1)$ spectra at the various observing positions. The temperature scale is in T_{mb} . We show only detections and suspected detections.

east-west nature of the emission is confirmed but the relative intensities of the east-west peaks requires further observations.

There is good overall agreement between the CO emission, the low-velocity $\text{H}\alpha$ emission, the dust, and the hot X-ray gas. All share an East-West extension and have a similar spatial extent. Like our $^{12}\text{CO}(2-1)$ distribution (Fig. 4a), both the X-ray emission (Bohringer et al. 1993) as well as the low-velocity $\text{H}\alpha$ emission (Unger et al. 1990) also display peaks on the eastern side of the nucleus. The radio map of Pedlar et al. (1990) with $\sim 5''$ resolution, is oriented at roughly 90 degrees to the CO and $\text{H}\alpha$ emission. As already mentioned, the radio emission seems to have displaced the X-ray emitting gas (cf. Figure 1 of Bohringer et al., where the ROSAT HRI image is overlaid on the radio contours); we return to this point in Section 5.2 and the Discussion.

Figure 4b shows a crude representation of the velocity field in the $^{12}\text{CO}(2-1)$ line, where we have measured the velocity at each of the positions in Figure 1, using the SPECX `find-centroid` task. Some of the spectra are low S/N, and we have indicated this in Figure 4b by enclosing the velocity in parentheses [e.g. (5140)]; we have used ‘...’ to indicate those positions for which no line was detected. Figure 4b indicates that, not only is the $^{12}\text{CO}(2-1)$ gas blueshifted at the (0,0) point, but all the gas over the mapped area is blueshifted by 100–150 km s^{-1} relative to the systemic velocity of the galaxy. (The same conclusion is reached if we instead plot the peak velocities using gaussian

fits to the spectra or whether we try different baseline subtractions.) This is in contrast to Reuter et al. (1993) who found evidence for rotation from their $^{12}\text{CO}(2-1)$ velocity field (their Figure 5), but from their individual $^{12}\text{CO}(2-1)$ spectra (their Figure 2), it is not clear if this rotation is significant. Our $^{12}\text{CO}(2-1)$ data show little evidence for rotation on the larger scales mapped. Since the central $^{13}\text{CO}(2-1)$ spectrum (Fig. 3) shows two peaks, consistent with the rotational components observed by Inoue et al. (1996), we find that any rotation, if present, appears to be confined to a central ring. We discuss this further in Section 6.2.

4 THE MOLECULAR GAS: LINE RATIOS AND EXCITATION CONDITIONS

4.1 Formation of Line Ratios

The IRAM $^{12}\text{CO}(2-1)$ (beam size = $12''$) and $^{12}\text{CO}(1-0)$ (beam size = $21''$) $\int T_{mb}dV$ quantities of Reuter et al. (1993) have been sampled in a $7''$ grid in the central regions and an $11''$ grid for the outer points. Their calibration error is estimated to be $\approx 10\%$ or lower for $^{12}\text{CO}(1-0)$ and $\approx 10 - 20\%$ for $^{12}\text{CO}(2-1)$ (Reuter, private communication). We interpolated these data using GILDAS in the same way as the JCMT data (see §3) and reproduced the maps of Reuter et al. (their Fig. 3 and Fig. 4). The data were then smoothed, as required, to a 21 arcsec gaussian beam.

For the JCMT $^{12}\text{CO}(3-2)$ data (beam size = $14''$), the

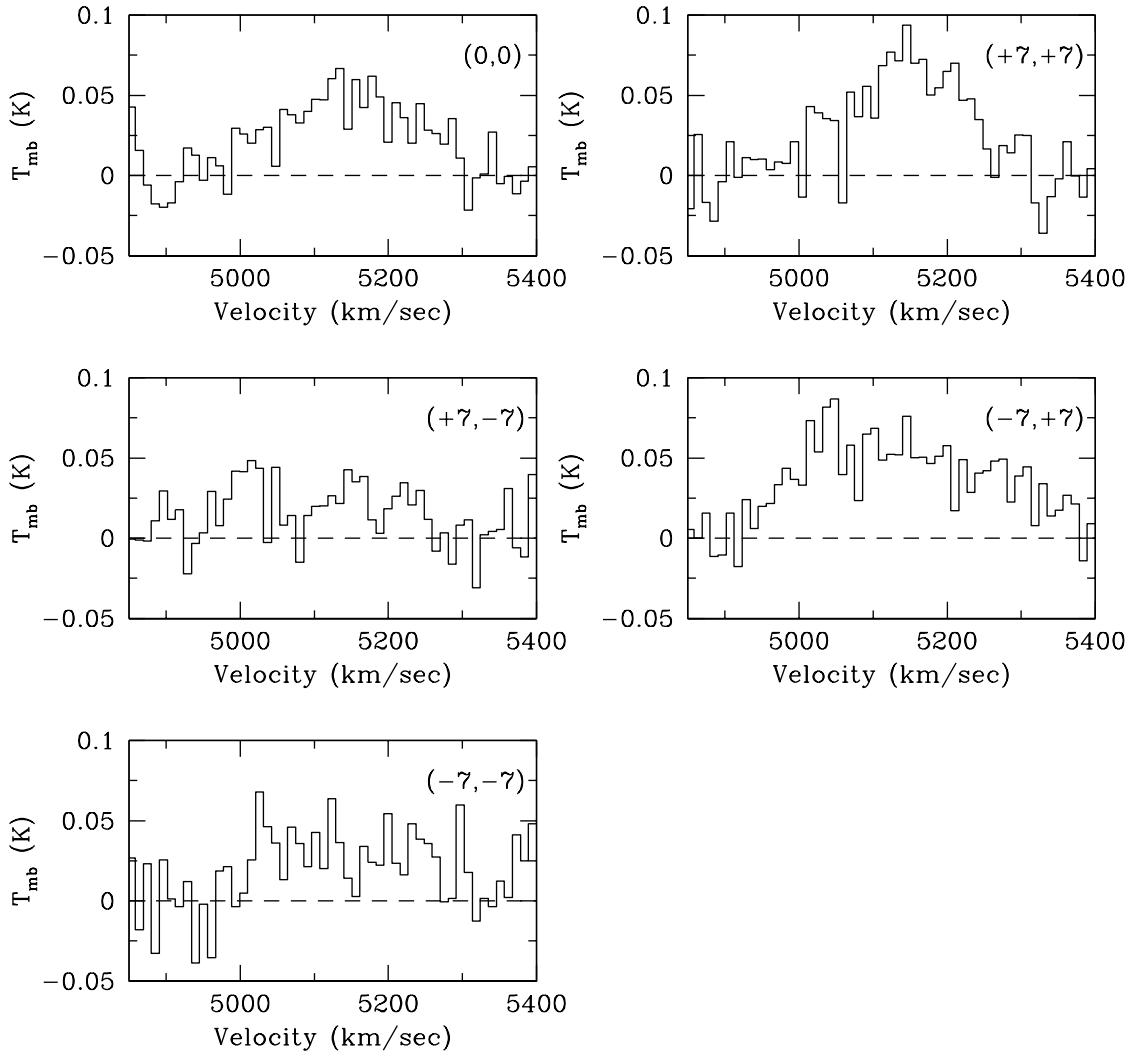


Figure 2. $^{12}\text{CO}(3-2)$ spectra immediately around the center

sampling was at 7 arcsec intervals covering a $28''$ region. These data were also interpolated and smoothed. For these data, it was also possible to form a line ratio over a smaller $14''$ beam, since the IRAM $^{12}\text{CO}(2-1)$ $12''$ resolution map could be smoothed to $14''$.

Since there was some redundancy in the observations (i.e. $^{12}\text{CO}(2-1)$ for both IRAM and the JCMT), we could also check on the reliability of the absolute calibration. To do this, we smoothed the interpolated $12''$ resolution IRAM $^{12}\text{CO}(2-1)$ map to $21''$ and directly compared the emission within $21''$ centered at (0,0) to the JCMT $^{12}\text{CO}(2-1)$ value at (0,0) in a $21''$ beam. The result is excellent (possibly fortuitous) agreement to within 5%.

The resulting line ratios for the (0,0) position are listed in Table 3, where we use the nomenclature, ${}^n\text{CO}(i-j) \equiv \int T_{mb}[{}^n\text{CO}(i-j)]dV$. The final error bars in the ratio are of order 15% to 50% and attempt to take reasonable account of noise in the spectra, differences introduced by subtracting different baselines or choosing different integration limits,

differences introduced by interpolation/sampling, and differences (where measured) between telescopes. In the case of $^{13}\text{CO}(2-1)$, we also include a measured variation between the ratio of integrated intensity and ratio of peak intensity (Fig. 3).

4.2 Discussion of Line Ratios

Our measured $^{12}\text{CO}(2-1)/^{12}\text{CO}(1-0)$ ratio of 0.74 ± 0.11 (Table 3) for the cD galaxy, NGC 1275, falls within the range normally observed for spiral galaxies. For example, the mean for optically selected nearby spirals is $^{12}\text{CO}(2-1)/^{12}\text{CO}(1-0) = 0.89 \pm 0.06$, with higher values (~ 1.1) measured for perturbed galaxies (Braine & Combes 1992; Braine et al. 1993). Values of 0.93 ± 0.22 are found for IR bright galaxies (Aalto et al. 1995) and > 1 for some starburst galaxies (Loiseau et al. 1990; Braine et al. 1993). Wilson, Walker, & Thornley (1997) find values ranging between 0.5 to 1.07 for specific molecular cloud regions in M33.

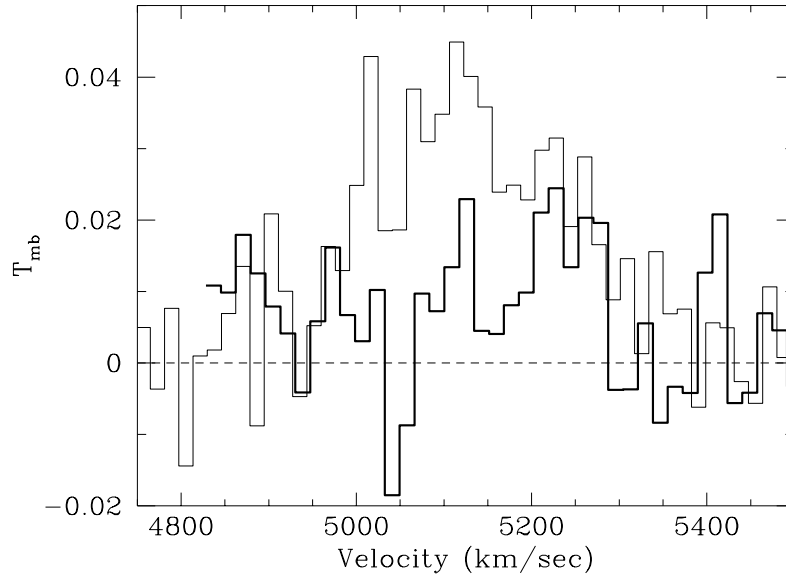


Figure 3. $^{13}\text{CO}(2-1)$ spectrum at the (0,0) position (heavy line) with the $^{12}\text{CO}(2-1)$ spectrum (light line) superimposed. The apparent increase in emission at the low velocity end of the spectrum is due to baseline curvature.

The isotopic ratio of $^{12}\text{CO}(2-1) / ^{13}\text{CO}(2-1) = 6 \pm 3$ (based on our marginal detection of $^{13}\text{CO}(2-1)$) is also typical of giant molecular clouds (GMCs), for example, values of 4 - 14 with a median of $\sim 5 - 6$ are found for this ratio in the Galaxy (Sanders et al. 1993) and Wilson, Walker, & Thornley (1997) find an average of 7 ± 1 for 7 molecular clouds in M33. Higher ratios tend to be found for starburst galaxies (e.g. 12 for M 82; Tilanus et al. 1991) and IR-bright and luminous mergers (> 20 for the CO(1-0) isotopic ratio; Aalto et al. 1995).

In contrast, our $^{12}\text{CO}(3-2) / ^{12}\text{CO}(2-1)$ of 1.25 ± 0.25 ($21''$ beam) is higher than normally observed in spirals. Typically, the $^{12}\text{CO}(3-2) / ^{12}\text{CO}(2-1)$ ratio is lower than $^{12}\text{CO}(2-1) / ^{12}\text{CO}(1-0)$. For example, Sanders et al. (1993) find $^{12}\text{CO}(2-1) / ^{12}\text{CO}(1-0)$ and $^{12}\text{CO}(3-2) / ^{12}\text{CO}(2-1)$ ratios of ~ 0.8 (ranging from ~ 0.7 to 0.95) and ~ 0.4 (ranging from ~ 0.35 to 0.7), respectively, for Galactic GMCs within the solar circle. Mean values for the nuclear region of IC 342 are 1.0 and 0.47 (Irwin & Avery 1992).

Thus our line ratios for the giant cD galaxy, NGC 1275 (Table 3) are not untypical of those observed for normal spiral galaxies, with the possible exception of the $^{12}\text{CO}(3-2) / ^{12}\text{CO}(2-1)$ ratio, which appears to be somewhat high. Similarly high values of $^{12}\text{CO}(3-2) / ^{12}\text{CO}(2-1)$ (i.e. 1.1 to 1.3) have also been observed by Wall et al. (1993) in a small sample of IR bright galaxies. They require a 2-component model to explain their data. We explore this possibility in the next section.

4.3 LVG Analysis and Cloud Properties

For a line ratio analysis, it is usually assumed that the observed main beam brightness temperature, $T_{mb\nu}(V)$, in a particular spectral line of frequency, ν , for a cloud moving at some velocity, V , is just the radiation temperature of the clouds, $T_{R\nu}(V)$ (see Kutner & Ulich 1981), diluted by a filling factor:

$$T_{mb\nu}(V) = ff\nu(V) * T_{R\nu}(V) \quad \text{--- [1]}$$

where the filling factor, $ff\nu(V)$, includes the area filling factor for clouds at velocity, V , and a filling factor in velocity (due to dilution within channels) if required.

In order to make use of the observed (integrated) line ratios (Table 3), it is necessary to assume that the emission from each line at velocity, V , is coming from equivalent regions within the beam, i.e. the filling factors for each line at velocity, V , are equivalent. This assumption also ensures that the ratios of integrated line strength (which have higher S/N) are equal to the ratios of peak $T_R(V)$ which is the modeled quantity.

We could check this assumption for the two cases for which the original (unsmoothed) beam sizes were identical. The first is the JCMT $^{12}\text{CO}(2-1)$ and IRAM $^{12}\text{CO}(1-0)$ data. A measurement of the peak $T_{mb}^{12}\text{CO}(2-1) / T_{mb}^{12}\text{CO}(1-0)$ ratio gives a result which agrees with the integrated ratio (Table 2) to within 5%, well within the quoted errors. The second is the JCMT $^{13}\text{CO}(2-1)$ and $^{12}\text{CO}(2-1)$ data. Since the $^{13}\text{CO}(2-1)$ line may be more optically thin than the $^{12}\text{CO}(2-1)$ line, this line ratio is more likely than the others to suffer from differing filling factors. This indeed appears to be the case, given the relative symmetry of

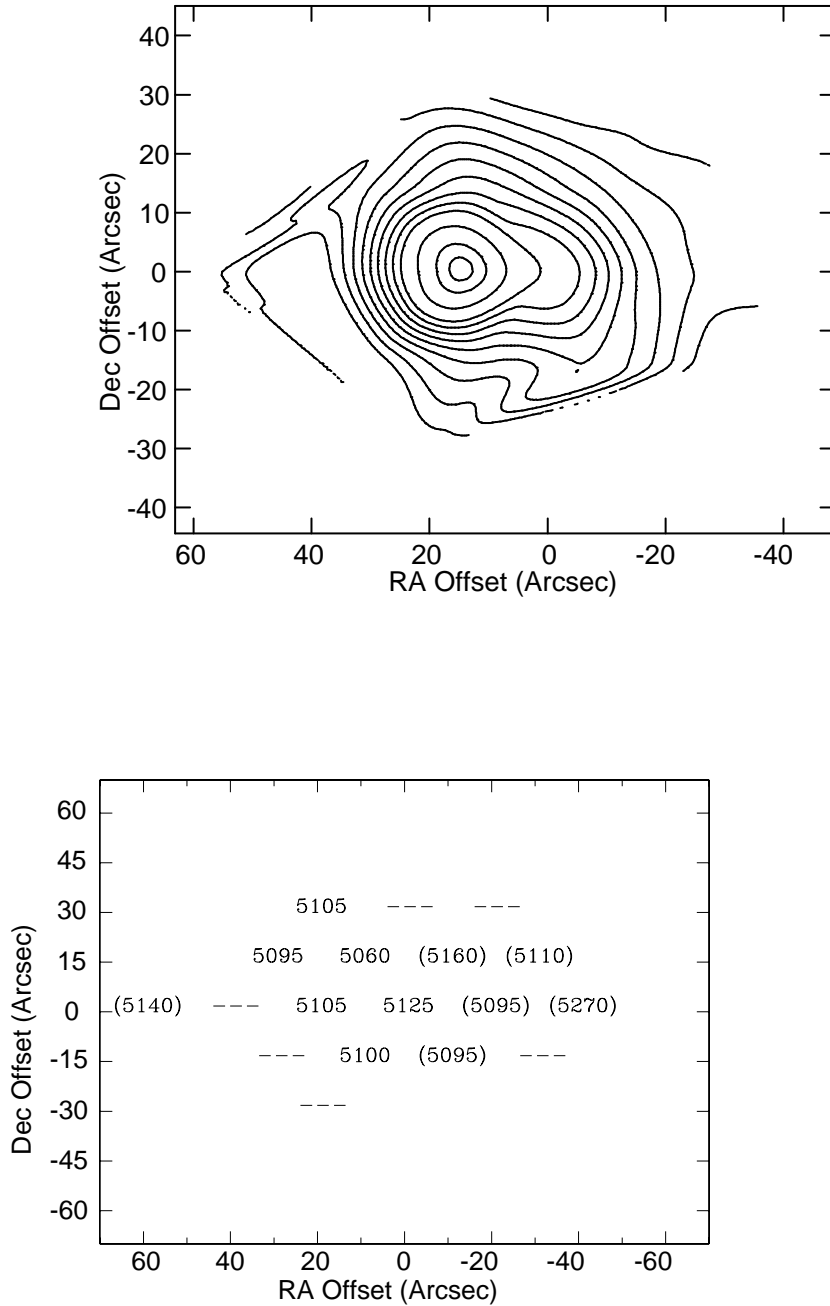


Figure 4. (a) Map of integrated intensities in $^{12}\text{CO}(2-1)$. Contour levels are at 1, 2, 3, 4, 5, 6, 7, 8, 9, 11, 13, and 14 K km s^{-1} . Structure around the extreme periphery is artificial due to interpolation into regions containing no data. (b) Crude Velocity Field in $^{12}\text{CO}(2-1)$. The velocity has been determined by finding the velocity centroids of each spectrum. Values enclosed in '()' have more uncertainty, and '—' indicates that there is no line detected at that position.

the $^{13}\text{CO}(2-1)$ line with respect to the systemic velocity, in contrast to the observed asymmetry of the $^{12}\text{CO}(2-1)$ line (§3.2). In this case, therefore, the error bar in the $^{12}\text{CO}(2-1)/^{13}\text{CO}(2-1)$ line ratio takes into account the variation between the ratio of peak T_{mb} and the ratio of integrated line strengths.

Thus, within the uncertainties quoted and the limita-

tions of what can be checked, the assumption of equivalent filling factors appears to be valid.

The line ratios of Table 3, applicable to a $21''$ beam, were considered in the context of the Large Velocity Gradient (LVG) approximation (Goldreich & Kwan 1974; De Jong, Chu, & Dalgarno 1975), following Irwin & Avery (1992) and using the collisional rates of Flower & Launay (1985) which are tabulated from 10 K to 250 K. An 11-

Table 2. Line Strengths at each Position

Position	Integration (sec)	T_{mb} (peak) (K)	ΔV (FWHM)	$\int T_{mb} dV$ (K km s ⁻¹)
¹²CO(3-2)				
(0,0)	3000	0.053	175	11.6 ± 0.95
(-7,+7)	2400	0.055	380	18.7 ± 1.4
(+7,+7)	2400	0.072	170	13.1 ± 1.2
(+7,-7)	2400	0.030	120	5.6 ± 1.5
(-7,-7)	2400	0.034	300	8.7 ± 1.4
¹³CO(2-1)				
(0,0)	5520	0.017	140	1.24 ± 0.36
¹²CO(2-1)				
(0,0)	3720	0.036	180	8.90 ± 0.90
(-10,+15)	1800	0.046	30	2.70 ± 1.00
(+10,+15)	2400	0.025	145	6.14 ± 1.06
(+10,-15)	2400	0.028	135	4.13 ± 0.90
(-10,-15)	2400	0.019	220	4.65 ± 1.03
(-20,0)	3600	0.020	95	2.71 ± 0.76
(+20,0)	3000	0.038	330	12.23 ± 1.00
(0,+30)	5400	< 0.025	—	< 1.8
(-30,+15)	5520	0.011	85	1.13 ± 0.41
(+30,+15)	4800	0.031	85	2.85 ± 0.28
(+30,-15)	5400	< 0.015	—	< 1.8
(-30,-15)	6690	< 0.015	—	< 1.8
(-20,+30)	6000	< 0.020	—	< 2.4
(+20,+30)	6000	0.018	65	1.20 ± 0.23
(+20,-30)	5400	< 0.025	—	< 3.0
(-40,0)	5400	0.013	50	1.39 ± 0.62
(+40,0)	3000	< 0.043	—	< 5.3
(+60,0)	1800	0.010	125	1.97 ± 0.61

Table 3. CO Line Ratios

Line Ratio	Beam FWHM	Value
¹² CO(3-2) / ¹² CO(2-1)	14''	1.0 ± 0.15
¹² CO(3-2) / ¹² CO(2-1)	21''	1.25 ± 0.25
¹² CO(2-1) / ¹² CO(1-0)	21''	0.74 ± 0.11
¹² CO(2-1) / ¹³ CO(2-1)	21''	6.0 ± 3.0

level CO molecule is assumed; the excitation temperature of the highest level is 305 K. Given a kinetic temperature, T_k , molecular hydrogen density, n_{H_2} , and fractional CO abundance, X , per unit velocity gradient, (dV/dr) , $X (dV/dr)^{-1}$, as inputs, the radiation temperature, T_R , optical depth, τ , and excitation temperature, T_{exc} , can be predicted for each line, as well as the line ratios. The input quantities can then be adjusted until the observed line ratios are reproduced.

This method makes as few assumptions as possible about the physical conditions in the gas (in comparison to, say, an LTE model), an approach which is particularly important for a cooling flow galaxy in which physical conditions may be atypical. This approach does, however, assume that the molecular clouds within the beam have equivalent physical properties. i.e. the beam-averaged line ratios provide us with mean beam-averaged physical properties of all clouds. We require only an isotopic abundance ratio which we take to be $I = [^{12}\text{CO}] / [^{13}\text{CO}] = 50 \pm 30$ (Langer &

Table 4. Best-Fit One-Component LVG Results

Parameter	With ¹³ CO(2-1)	Without ¹³ CO(2-1)
T_{kin} (K)	30	20
n_{H_2} (cm ⁻³)	1×10^3	3×10^3
$X (dV/dr)^{-1} (\text{km s}^{-1} \text{pc}^{-1})^{-1}$	1×10^{-4}	1×10^{-4}
I	80	—
$T_R[^{12}\text{CO}(3-2)]$ (K)	16.5	12.5
$T_R[^{12}\text{CO}(2-1)]$ (K)	20.6	14.6
$T_R[^{13}\text{CO}(2-1)]$ (K)	2.7	—
$T_R[^{12}\text{CO}(1-0)]$ (K)	22.7	16.4
$\tau[^{12}\text{CO}(3-2)]$	42.3	148
$\tau[^{12}\text{CO}(2-1)]$	29.9	130
$\tau[^{13}\text{CO}(2-1)]$	1.5	—
$\tau[^{12}\text{CO}(1-0)]$	10.1	48.7
$T_{exc}[^{12}\text{CO}(3-2)]$ (K)	23.9	19.7
$T_{exc}[^{12}\text{CO}(2-1)]$ (K)	26.0	19.8
$T_{exc}[^{13}\text{CO}(2-1)]$ (K)	8.0	—
$T_{exc}[^{12}\text{CO}(1-0)]$ (K)	26.2	19.9
¹² CO(3-2) / ¹² CO(2-1)	0.80	0.86
¹² CO(2-1) / ¹² CO(1-0)	0.91	0.89
¹² CO(2-1) / ¹³ CO(2-1)	7.6	—

Penzias 1990; also van Dishoeck & Black 1988). A velocity model of the individual clouds is also required. In practise, the choice of velocity model is not critical, given the uncertainties of the data; here we assume uniformly collapsing clouds (cf. Richardson 1985).

We searched through parameter space over a range of density from 10^3 to 10^8 cm^{-3} and abundance per unit velocity gradient from 10^{-10} to $10^{-2} (\text{km s}^{-1} \text{pc}^{-1})^{-1}$, both in steps of $10^{n/2}$, n an integer, kinetic temperature from 10 K to 250 K in steps of 10 K, and for isotopic abundance ratios of 20, 50, and 80. The best-fit (from a χ^2 test) one-component results are listed in Table 4, column 2. Since the ¹³CO(2-1) line was only a marginal detection, we then repeated this process, excluding this line. These results are listed in Table 4, column 3.

From Table 4, we find similar results, regardless of the inclusion of the isotopic line ratio, except for τ . The results suggest the presence of cold (20 - 30 K) clouds of low (10^3 cm^{-3}) density. A comparison between the predicted line ratios of Table 4 (last 3 rows) and the observed values of Table 3, however, shows that even the best-fit result does not reproduce the observed ¹²CO(3-2) / ¹²CO(2-1) and ¹²CO(2-1) / ¹²CO(1-0) ratios to within the quoted errors. Again, if the isotope is excluded, the agreement is still poor. We cannot exclude the possibility that systematic errors may be present, causing us to underestimate the uncertainties of Table 3. However, given the unusual environment of NGC 1275 (e.g. the presence of the radio core, and the possibilities of the cooling flow and past interaction), and considering the beam size ($21'' = 7.14 \text{ kpc}$), we feel it is more likely that the clouds in the centre of this galaxy cannot be described by a one-component model.

A simple two-component model could be described in which two types of clouds, A and B, are allowed, each with a unique value of $n(\text{H}_2)$, $X (dV/dr)^{-1}$, T_{kin} and filling factor. Equation [1] could then be replaced by:

$$T_{mb\nu} = ff_A * T_{RA\nu} + ff_B * T_{RB\nu} \dots [4]$$

and the line ratios then computed as before. We have indeed developed such an LVG model which can accommodate two

components. However, this two-component model now has 7, rather than 3, free parameters and we no longer have sufficient data to solve for these parameters. We have, nevertheless, searched through parameter space (where we have allowed the filling factor of component B compared to A to range in steps of $10^{n/4}$, n an integer from -25 to 0) to see if there are regimes which can be excluded.

With a two-component fit, it is possible to match the observed line ratios quite well within error bars. As expected, the results for the two-component model are generally unconstrained and solutions are found over the entire range of density, temperature and filling factor. However, the one conclusion that can be reached from the two-component analysis is that *it is not possible to find a solution for which the two cloud components have the same temperature*. Varying the density, filling factors, and/or abundance per unit velocity gradient between the two components with a single temperature cannot reproduce the observed line ratios. (This conclusion remains, if the isotopic ratio is excluded from the analysis.) Our best (but non-unique) two-component model which shows the *least* difference in kinetic temperature has a cold (10 K) Component A at a density of $1.0 \times 10^3 \text{ cm}^{-3}$ and a hot (170 K) Component B at a density of $3.1 \times 10^4 \text{ cm}^{-3}$ with the filling factor of the hot component about half that of the cold component. Thus the simplest interpretation of the results is that temperature gradients occur in the molecular gas within the central $21''$ of NGC 1275. This will be discussed further in Section 6.

5 QUANTITY AND PRESSURE OF THE MOLECULAR GAS

5.1 Total Molecular Gas Mass

We have estimated the total molecular (H_2) gas in the usual way, using a Galactic conversion between CO intensity and M_{H_2} :

$$M_{\text{H}_2} = 5.82 \times 10^6 I_{\text{CO}(1-0)} (\pi/4) d^2 \quad ,$$

where d is the telescope beam diameter in kpc at the source distance (here $d=7.1$ kpc for $D=70$ Mpc within our $21''$ beam). The numerical factor is taken from Sanders, Solomon, & Scoville (1984), and is applicable for the CO(1–0) transition. We follow McNamara & Jaffe (1994) and use the above equation for other transitions by multiplying the numerical factor by the appropriate line ratios taken from Table 3. Our results can be summarized as $M_{\text{H}_2} = 2.8 \times 10^9 M_{\odot} \pm (8-10) \times 10^8 M_{\odot}$ for the $^{12}\text{CO}(1-0)$, $^{12}\text{CO}(2-1)$, and $^{12}\text{CO}(3-2)$ transitions, where uncertainties in both the distance and the line ratios have been accounted for; *no* uncertainty has been assumed in the Sanders, Solomon, & Scoville CO(1–0) numerical factor. A similar result is found for the weaker $^{13}\text{CO}(2-1)$ transition, but with a correspondingly larger uncertainty. The total mass over all emission mapped (shown by Fig. 4a, Table 2) is $M_{\text{H}_2} = 1.6 \times 10^{10} M_{\odot}$.

We can compare our M_{H_2} mass of $\sim 3 \times 10^9 M_{\odot}$ within our central $21''$ beam directly with that of Lazareff et al. (1989), and Reuter et al. (1993) who observed NGC 1275 with the 30m IRAM telescope in the $^{12}\text{CO}(1-0)$ transition

with the same beamsize, and found $M_{\text{H}_2} = 6 \times 10^9 M_{\odot}$ (all comparisons are made assuming a distance of 70 Mpc and adjusted to our conversion factor) and $2.7 \times 10^9 M_{\odot}$, respectively. The latter authors find a total mass of $M_{\text{H}_2} = 8.6 \times 10^9 M_{\odot}$ over their total mapped region (a total area of $\sim 40'' \times 30''$ which is smaller than that shown in Fig. 5). Mirabel, Sanders, & Kazes (1989) obtained $^{12}\text{CO}(1-0)$ data with the 12m NRAO telescope, and found $M_{\text{H}_2} = 3.2 \times 10^9 M_{\odot}$ within their $55''$ beam. Finally, Inoue et al. (1996) find M_{H_2} of 8.6×10^9 and $4.3 \times 10^{10} M_{\odot}$ within diameters of $9''$ and $65''$ respectively. Thus, our M_{H_2} mass is comparable with most previous single dish measurements, though the interferometer data give higher results.

We must stress that the above determinations of the molecular gas mass have relied upon a Galactic conversion between M_{H_2} and CO integrated intensity. Conditions in cluster cooling flows are likely to be very different from those of Galactic molecular clouds, and the conversion factor may depend on such factors as metallicity and the intensity of the UV radiation field (e.g. Wilson 1995; Arimoto, Sofue, & Tsujimoto 1996). Further observational and theoretical work is needed to determine the conversion factor over the full range of environments encountered (early and late type galaxies, starbursts, cooling flows, etc.).

5.2 Gas Pressure

Unfortunately we cannot compute the pressure of the molecular gas with certainty because we have only rough constraints on the gas temperature and density from our LVG analysis (§4.5). However, we can use the values from our best two-component solution (Section 4.3) to provide a sample solution. Taking $T_{\text{kin}}=170$ K and $n_{\text{H}_2} = 3 \times 10^4 \text{ cm}^{-3}$ for the hot, dense Component B (the pressure from Component A can be ignored), we find a molecular gas pressure $P \simeq 7 \times 10^{-10} \text{ erg cm}^{-3}$. Since Component B's density is reasonably well constrained and its tabulated temperature is a lower limit (§4.3), this result should represent a rough lower limit, in the context of the two-component LVG model. Bohringer et al. (1993) quote a pressure for the hot X-ray emitting gas in the central region of Perseus of $2.5 \times 10^{-10} \text{ erg cm}^{-3}$, while C. Peres (private communication) finds $P \sim 2.5 \times 10^{-9} \text{ erg cm}^{-3}$ at a radius of $8''$, both from ROSAT HRI data (and both values corrected to $H_0=75$). The latter number is the best to compare with our value, and the agreement is reasonable given the uncertainties in both our LVG analysis and the X-ray determinations near the cluster center. We can also compare with the pressure found for the optical [SII] emission lines by Heckman et al. (1989): $P_{\text{opt}}=7 \times 10^{-10} \text{ erg cm}^{-3}$ between 2–5 kpc (6–15''). Thus, there is good agreement between the gas pressures as determined from X-ray, sub-mm, and optical data.

Bohringer et al. (1993) overlaid their ROSAT HRI image of Perseus with the 332 MHz radio data of Pedlar et al. (1990), and found that the X-ray gas and radio plasma are anti-correlated. In particular, the outer radio lobes are coincident with minima in the X-ray surface brightness, and Bohringer et al. speculated that the radio plasma has displaced the thermal gas. Similar results are found for other clusters with lobe-dominated radio sources, including Abell 1795, 2029, 2597 and 4059 (see Sarazin 1997 for references),

Abell 2634 (Schindler & Prieto 1997), and Abell 2199 (Owen & Eilek 1997).

6 DISCUSSION

6.1 Displacement of the Molecular Gas by the Radio Plasma?

We indicated in Section 5.2 that the radio lobes and thermal gas have similar pressures, and that the radio lobes and X-ray gas avoid each other. Following Bohringer et al. (1993), we speculate that the radio lobes are thus displacing the hot X-ray gas, the optical line-emitting gas, *and* the molecular gas. If the molecular gas on the side of the galaxy nearest to us is being pushed outwards, this could explain the blueshift of 100–150 km s⁻¹ we observe in the ¹²CO(2–1) and ¹²CO(3–2) emission. We now show that this idea can also work energetically.

Roughly speaking, the kinetic energy needed to displace the $\sim 1.6 \times 10^{10} M_{\odot}$ ($\times 1.4$ to account for heavier elements) of molecular gas at a velocity of 150 km s⁻¹ is $\sim 5 \times 10^{57}$ ergs; compare this with the total (minimum) energy in the radio halo (Component A) of 3×10^{57} ergs determined by Pedlar et al. (1990). The latter radio value applies to a region $38'' \times 15''$ in size and would actually be higher over a region which is comparable to the molecular gas component [Fig. 4(a)] since more radio emission is present on larger scales. A simple linear scaling for area gives a modified radio energy of $\sim 16 \times 10^{57}$ ergs, or a factor of ~ 3 higher than the molecular gas kinetic energy in the same region. Thus (depending on the efficiency of energy transfer and given the uncertainties) there appears to be sufficient energy in the radio components to account for the velocity displacement of the molecular gas.

Note that it is unlikely that the blueshifted emission represents gas on the far side of the nucleus which is infalling as a result of the cooling flow because velocities as high as 150 km s⁻¹ are not expected for quasistatically contracting cooling flow gas.

6.2 What’s Special About NGC 1275?

Why is NGC 1275/Perseus the only cooling flow cluster with detected CO emission? The best upper limits on M_{H_2} are already a few times $10^9 M_{\odot}$ (e.g. McNamara & Jaffe 1994; Braine & Dupraz 1994; O’Dea et al. 1994), and there are at least 14 clusters which would have been detected in CO if they contained quantities of molecular gas similar to that found in NGC 1275/Perseus. As we discussed in the Introduction, there have been detections of excess X-ray absorption in many clusters (White et al. 1991; Allen & Fabian 1997). While the physical properties of this absorbing material are not at all known (see discussion in Sarazin 1997), it has been argued that much of it might consist of very cold (~ 3 K) and dense molecular clouds. However, NGC 1275 happens to have one of the strongest radio cores of any cooling flow central galaxy. This radio core may heat the molecular gas to detectable temperatures in NGC 1275/Perseus, while the gas remains cold in most other clusters. As we have discussed already, the radio plasma is certainly affecting the thermal gas on larger scales.

There are other possibilities. Braine et al. (1995) point out that “The FIR and CO emission from NGC 1275 correspond exactly to what is found in gas-rich spirals. Rather than a massive cooling flow, the gas may come from accretion of one or more gas-rich galaxies.” There is evidence for a past merger or interaction in NGC 1275 from the shells and young globular clusters seen in HST images (note, for instance, that NGC 1275 is probably suffering an interaction with the high-velocity system seen in absorption). In this case, the molecular gas would be much warmer and hence detectable. As well, the gas could be heated up during the merger event itself. Mergers appear to be rare in rich clusters at the present epoch, given their large velocity dispersions (e.g. Merritt 1985), and this is consistent with the non-detections of CO in other cooling flow clusters. A merger of a dust and gas rich spiral could also be the source of the thermal emission from dust observed in NGC 1275 (e.g. Lester et al. 1995).

7 SUMMARY

NGC 1275 is a remarkable galaxy with properties not seen anywhere else. With its central position in the Perseus cooling flow, its young blue globular clusters, the evidence for a past merger, the foreground infalling system, and its molecular gas component, it is so far unique amongst all galaxies, not just those of its class. Here we have focussed on the molecular gas distribution in NGC 1275, since this is the *only* cooling flow galaxy (so far) which displays a cold molecular component. Using the JCMT, we have mapped the ¹²CO(2–1) distribution of this galaxy at a resolution of 21'', detecting gas out to radii of 36'' (12 kpc). Within the limitations of our spatial resolution and coverage, we find an approximate east-west orientation to the emission, consistent with that found by previous authors in H α emission, X-ray emission, and the dust component. Evidence for the inner molecular rotating disk is also seen, consistent with NMA interferometric data. However, on broader scales we see no evidence for rotation.

The CO line profiles are consistently bluewards asymmetric, both at the central position in both ¹²CO(3–2) and ¹²CO(2–1) and over the entire region mapped in ¹²CO(2–1), where the S/N is sufficient to measure this quantity. We interpret this blueshift as being due to kinetic energy imparted by the radio jet/outflow in the advancing direction on the near side of the nucleus. With an estimate of total H₂ mass (assuming Galactic conversion factors) of $1.6 \times 10^{10} M_{\odot}$, and velocity offset of 150 km s⁻¹, we find that $\sim 5 \times 10^{57}$ ergs is required to impart this kinetic energy. There appears to be sufficient energy in the radio source to account for this, given the uncertainties. This result is consistent with Bohringer et al. (1993) who found that the X-ray gas has been displaced by the radio jet. No corresponding redshifted component is seen, possibly because the (receding) radio jet is less active.

Together with additional JCMT ¹³CO(2–1) data as well as ¹²CO(2–1) and ¹²CO(1–0) IRAM data from Reuter et al. (1993), we have formed three line ratios applicable to a central 21'' beam. Two of the line ratios appear to be typical of cold Galactic clouds, but the third [¹²CO(3–2) / ¹²CO(2–1)] is suggestive of gas under more “active”, warmer condi-

tions. This is confirmed by an LVG radiative transfer analysis which indicates that the observed line ratios cannot be reproduced by a single component, i.e. a single set of kinetic temperature, molecular hydrogen density, and abundance per unit velocity gradient. We have therefore developed a simple two-component model to describe the data. In the two-component analysis, there are insufficient line ratios to fully constrain the set of cloud parameters; however, the results indicate that the observed line ratios can be reproduced if the two molecular components are at different temperatures. It may be that a temperature gradient exists in the central region possibly due to the radio core.

Finally, while we note that the characteristics of the molecular gas in NGC 1275 have been readily related to the nuclear radio activity, these observations do not allow us to rule out a possible connection with the cooling flow, itself.

ACKNOWLEDGEMENTS

The authors wish to thank Dr. Lorne Avery and Jessica Arlett for providing the initial LVG code. We are grateful to H.-P. Reuter and his collaborators for sharing their IRAM data, and to Clovis Peres for showing us his ROSAT analysis before publication. We appreciate very much the assistance we received from our Support Astronomer Chris Purton, and Bill Dent, Per Friberg, and Tim Jenness who carried out remote observing for us in December 1995. Thanks to Henry Matthews for answering many questions relating to the calibration of our data. Thanks finally to Rachael Padman for all of her work in developing the SPECX package, and for helping us to use it. We thank the anonymous referee for a thorough reading of the paper, and suggestions for improvement. This work has been supported by Natural Sciences and Engineering Research Council of Canada Grant # OGP0184201 (for JI).

REFERENCES

- Aalto S., Booth R.S., Black J.H., Johansson L. E. B., 1995, *A&A*, 300, 369
- Allen S. W., Fabian A. C., Johnstone R. M., Nulsen P. E. J., Edge A. C., 1992, *MNRAS*, 254, 51
- Allen S.W., Fabian A.C., 1997, *MNRAS*, 286, 583
- Annis J., Jewitt D., 1993, *MNRAS*, 264, 593
- Arimoto N., Sofue Y., Tsujimoto, T., 1996, *PASJ*, 48, 275
- Bohringer H., Voges W., Fabian A. C., Edge A. C., Neumann D. M., 1993, *MNRAS*, 264, L25
- Braine J., Combes F., 1992, *A&A*, 264, 433
- Braine J., Combes F., Casoli F., Dupraz C., Gerin M., Klein U., Wielebinski R., Brouillet N., 1993, *A&AS*, 97, 887
- Braine J., Dupraz C., 1994, *A&A*, 283, 407
- Braine J., Wyrowski F., Radford S. J. E., Henkel C., Lesch H., 1995, *A&A*, 293, 315
- Calet A., Woodgate B.E., Brown L.W., Gull T.R., Hintzen P., Lowenthal J.D., Oliverson R.J., Zeigler M.M., 1992, *ApJ*, 388, 301
- Cowie L. L., Fabian A. C., Nulsen P. E. J., 1980, *MNRAS*, 191, 399
- De Jong T., Chu S. I., Dalgarno A., 1975, *ApJ*, 199, 69
- Edge A.C., Stewart G.C., Fabian A.C., 1992, *MNRAS*, 258, 177
- Fabian A. C., Hu E. M., Cowie L. L., Grindlay J., 1981, *ApJ*, 248, 47
- Fabian A. C., Nulsen P. E. J., Canizares C. R., 1982, *MNRAS*, 201, 933
- Fabian A.C., 1994, *ARA&A*, 32, 277
- Fabian A.C., Arnaud K.A., Bautz M.W., Tawara Y., 1994, *ApJ*, 436, 63
- Fischer J., Geballe T. R., Smith H. A., Simon M., Storey J.W.V., 1987, *ApJ*, 320, 667
- Flower D. R., Launay J. M., 1985, *MNRAS*, 214, 271
- Goldreich J., Kwan J., 1974, *ApJ*, 191, 93
- Gorenstein P., Fabricant D., Topka K., Harnden F. R., Tucker W. H., 1978, *ApJ*, 224, 718
- Grabelski D.A., Ulmer M. P., 1990, *ApJ*, 355, 401
- Heckman T.M., Baum S.A., van Breugel W.J.M., McCarthy P., 1989, *ApJ*, 338, 48
- Holtzman J. A., Faber S. M., Shaya T. R., et al., 1992, *AJ*, 103, 691
- Hu E.M., Cowie L.L., Kaaret P., Jenkins E.B., York D.G., Roesler F.L., 1983, *ApJ*, 275, 27
- Inoue M.Y., Kamenno S., Kawabe R., Inoue M., Hasegawa T., Tanaka M., 1996, *AJ*, 111, 1852
- Irwin J. A., Avery L. W., 1992, *ApJ*, 388, 328
- Jaffe W., 1990, *A&A*, 240, 254
- Jaffe W., 1992, in *Clusters and Superclusters of Galaxies*, ed. A. C. Fabian (Kluwer: Dordrecht), pg. 109
- Johnstone R.M., Fabian A.C., Edge A.C., Thomas P.A., 1992, *MNRAS*, 255, 431
- Kawara K., Taniguchi Y., 1993, *ApJ*, 410, L19
- Kutner M. L., Ulich B. L., 1981, *ApJ*, 250, 341
- Langer W. D., Penzias A.A., 1990, *ApJ*, 357, 477
- Lazareff B., Castets A., Kim D.-W., Jura M., 1989, *ApJ*, 336, L13
- Lester D. F., Zink E. C., Doppmann G. W., et al., 1995, *ApJ*, 439, 185
- Loiseau N., Nakai N., Sofue Y., Wielebinski R., Reuter H.-P., Klein U., 1990, *A&A*, 228, 331
- Lynds B., 1970, *ApJ*, 159, L151
- McNamara B. R., O'Connell R. W., 1992, *ApJ*, 393, 579
- McNamara B. R., Jaffe W., 1994, *A&A*, 281, 673
- Merritt D., 1985, *ApJ*, 289, 18
- Minkowski R., 1957, in *Radio Astronomy*, IAU Symp. 4, ed. H. C. van der Hulst (Cambridge, Cambridge University Press), p. 104
- Mirabel I. F., Sanders D. B., Kazes I., 1989, *ApJ*, 340, L9
- Mushotzky R. F., Holt S. S., Boldt E.A., Serlemitsos P.J., Smith B. W., 1981, *ApJ*, 244, L47
- O'Dea C.P., Baum S.A., Maloney P.R., Tacconi L.J., Sparks W.B. 1994, *ApJ*, 422, 467
- Owen F.N., Eilek J.A., 1997, astro-ph 9708140
- Pedlar A., Ghataure H. S., Davies R. D., Harrison B. A., Perley R., Crane P. C., Unger S. W., 1990, *MNRAS*, 246, 477
- Readhead A. C. S., Hough D. H., Ewing M. S., Walker R. C., Romney, J. D., 1983, *ApJ* 265, 107
- Reuter H.-P., Pohl M., Lesch H., Sievers A. W., 1993, *A&A*, 277, 21
- Richardson, K. J. 1985, Ph.D. Thesis, Department of Physics, Queen Mary College, University of London
- Sanders D.B., Solomon P.M., Scoville N.Z., 1984, *ApJ*, 276, 182
- Sanders D. B., Scoville N. Z., Tilanus R. P. J., Wang Z., Zhou, S., 1993, in *Back to the Galaxy*, AIP Conf. Proc. 278, ed. S. S. Holt and F. Verter (New York, American Institute of Physics), p. 311
- Sarazin C.L., 1997, in *Galactic and Cluster Cooling Flows*, ed. N. Soker, (San Francisco: Publ. Astr. Soc. Pacific), pg. 172
- Schindler S., Prieto M.A., 1997, *A&A*, 327, 37
- Tilanus R. P. J., Tacconi L. J., Sutton E. C., Zhou S., Sanders

- D. B., Wynn-Williams C. G., Lo K. Y., Stephens S. A., 1991, ApJ, 376, 500
Unger S.W., Taylor K., Pedlar A., Ghataure H.S., Penston M.V., Robinson A., 1990, MNRAS, 242, 33P
van Dishoeck E. F., Black J. H., 1988, ApJ, 334, 771
Wall W. F., Jaffe D. T., Bash F. N., Israel F. P., Maloney P. R., Baas F., 1993, ApJ, 414, 98
White D. A., Fabian A. C., Johnstone R. M., Mushotzky R.F., Arnaud K.A., 1991, MNRAS, 252, 72
Wilson C.D. 1995, ApJ, 448, 97
Wilson C.D., Walker C.E., Thornley M.D., 1997, ApJ, 483, 210